

Late-forming black holes and the antiproton, gamma-ray, and anti-helium excesses

Mrunal Korwar,^{a,c} Stefano Profumo^b

^aDepartment of Physics, University of California, Berkeley, CA 94720, USA

^bDepartment of Physics and Santa Cruz Institute for Particle Physics,
University of California, Santa Cruz, CA 95064, USA

^cDepartment of Physics and Astronomy, University of Kentucky, Lexington, KY
40506, USA

E-mail: mkorwar@berkeley.edu, profumo@ucsc.edu

Abstract. Black holes long-lived enough to be the dark matter have temperatures below the MeV. Since Hawking evaporation is a quasi-thermal process, no GeV emission is predicted to be produced by black holes if they are part, or all, of the cosmological dark matter. However, black holes could be “spawned” at late times with masses that correspond to short lifetimes, and as such be significantly hotter and produce particles well in excess of the GeV. Here, we show that such late-forming black holes could, at once, explain the tantalizing excesses found in the gamma radiation from the Galactic center, in the flux of cosmic-ray antiproton, and in the few tentative antihelium events reported by the anti-matter spectrometer AMS-02. We compute accurate predictions for the anti-deuteron, high-energy neutrino, and positron fluxes if this scenario is realized in nature. We find that while the neutrino and positron fluxes are too small compared to the expected background, a significant number of anti-deuteron events is expected both at AMS-02 and at the future General AntiParticle Spectrometer (GAPS).

Contents

1	Introduction	1
2	Best Fit Models for Late-Forming Black Holes	3
3	Model Predictions: antideuterons, positrons, neutrinos, and gamma rays	6
4	Discussion and Conclusions	8

1 Introduction

The nature of the cosmological dark matter (DM), posited in the standard cosmological model, remains elusive (for a constantly updated review, see Chapter 27 of [1]). The paradigm of weakly interacting particles (WIMPs), one where the DM is a weak-scale particle coupled, however weakly, typically in fact via weak interactions, to Standard Model particles, was considered for a long time as one of the most promising frameworks; as a result, a vast program of direct, indirect, and collider searches for WIMPs was undertaken, yielding, however, mostly negative results (see e.g. [2, 3] for an extensive review of the WIMP paradigm). Nevertheless, a few tantalizing anomalies, which we refer to as “excesses”, have been reported over the years that could potentially be ascribed to new physics effects sourced by a DM particle (for a pedagogical and complete review of indirect DM detection and the excesses described below see especially Ref. [4]).

One of the most persistent and intriguing example of such “excesses” is the Galactic center excess, which refers to an excess at a few GeV energies in the Fermi Large Area Telescope (LAT) [5] data over the expected diffuse gamma radiation in the inner Galaxy, originally discovered in Ref. [6, 7]. A significant debate followed, spurred by the potential contributions of unresolved point sources, a possible background mis-modeling due to the lack of time-dependent effects or the localization of the cosmic-ray sources, or the very templates used to build a model of the diffuse emission, among other possibilities (we refer the Reader for details to the comprehensive chapter 6 of Ref. [4]). Here, we use the results for the extrapolation of the Galactic center excess of three compelling analyses, including from the Fermi-LAT Collaboration [8, 9], as well as from Ref. [10], and the recent Ref. [11]¹.

A second excess we will focus our study on is a possible anomaly in the flux of cosmic-ray antiprotons in the 10-20 GeV energy range as measured by the anti-matter spectrometer AMS-02 [12], first discovered in Ref. [13, 14] and more firmly established in Ref. [15]. Here as well a lively debate ensued the claim that the excess could be associated with new physics, due to persistent issues with background modeling, source

¹We thank Mattia Di Mauro for kindly sharing with us his numerical results.

characterization, modeling of the propagation and of the interaction cross sections responsible for antiproton production and detection (again, we refer the interested Reader to section 5.2 of Ref. [4]). Here, we utilize the results of Ref. [15] when we refer to the “antiproton excess”.

Finally (albeit, alas, by no means is this a complete list of indirect detection excesses!) here we also consider the tantalizing report of potentially several anti-helium (${}^3\bar{\text{He}}$) events by AMS-02 [16, 17] (see also [this recent presentation](#)). Virtually absent any expected astrophysical background [16], the reported events could, however, originate from a misidentified matter ${}^3\text{He}$ nucleus – the latter being over 10^9 more frequent; the needed detector simulations that would help establish the mis-identification rate, and assess whether or not it is better than one part in a billion, are currently underway. In view of the possible contamination we entertain, here that only a fraction of the reported candidate events actually consists of ${}^3\bar{\text{He}}$.

While other studies have addressed some or multiple of the three anomalies described above, here, for the first time, we entertain the possibility that all three be connected with late-forming, small black holes of non-stellar origin (we will refer to them, following [18, 19], as micro-structure black holes (MSBH)). If black holes of non-stellar origin are to be a component, or all, of the cosmological DM, their lifetime must exceed the age of the universe (in fact, the constraints on the lifetime are significantly more stringent, see Ref. [20] for a recent study). Given that, absent new, beyond the Standard Model, degrees of freedom, the lifetime τ of a black hole of mass M is

$$\tau(M) \simeq t_U \left(\frac{M}{10^{15} \text{ gm}} \right)^3, \quad (1.1)$$

black holes need to be more massive than around $M \gtrsim 10^{15}$ gm (in fact, if black holes are to be most of the cosmological dark matter, their mass must exceed $M \gtrsim 3 \times 10^{17}$ gm, and even if they are only a small fraction, say 10^{-3} , constraints from the diffuse gamma-ray emission constrain the smallest possible mass $M \gtrsim 1 \times 10^{17}$ gm, see, again, Ref. [20]).

Black holes of mass M have a temperature [21]

$$T_{\text{BH}} = \frac{1}{8\pi G_N M} \simeq 1.06 \text{ MeV} \left(\frac{10^{16} \text{ gm}}{M} \right), \quad (1.2)$$

thus, if black holes are abundant, and primordial, their temperature must be below the MeV. Since Hawking radiation is a quasi-thermal process, the production of particles with energies in the multi-GeV range is exponentially suppressed and essentially absent.

However, black holes can be much lighter, and hotter, if they were produced in the *late universe*, or if they are *currently* being produced. Notable possible formation scenarios for such MSBH include, but are not limited to, the collapse of DM structures consisting of particles interacting via Yukawa forces, or the collapse of Q-balls or Fermi balls. Depending on the timescale for collapse, the resulting MSBH can form at different times in the universe, including now. In particular, Ref. [22], [23] and [24] consider the collapse of false vacuum remnants in first-order phase transitions arising

if particles develop large mass gaps between the two phases and become trapped in the early phase; Ref. [25] explores a formation scenario where primordial DM halos could be generated during radiation domination by long-range “fifth-forces” stronger than gravity; Ref. [26] and [27] study a similar possibility based, however, on a long-range Yukawa force, as does Ref. [28], albeit in a slightly different realization; Ref. [29] considers instabilities in the density perturbations of a strongly interacting fermion-scalar fluid where the sound speed turns imaginary, leading to exponential growth at sub-Compton scales; finally, Ref. [30] and [31] entertain the possible formation of black holes from the collapse of Fermi balls.

Here, we revisit and expand the idea put forth in [19], that MSBH may explain the GeV gamma-ray excess from the Galactic center, and explore the tantalizing possibility that, in fact, such excess can be explained *in concert* with the above-mentioned antiproton and anti-helium cosmic-ray anomalies as well. To explore this possibility, we first calculate in detail, in sec. 2, the spectrum of gamma rays, antiprotons and anti-helium nuclei expected from MSBH with temperatures in the 10 GeV range, and thus masses around 10^{12} gm; we then fit the MSBH mass and the rate at which such objects should form today to the three anomalies; in sec. 3 we crucially compute the expected spectrum of other cosmic-ray species, such as neutrinos, positrons, and anti-deuterons, expected if this scenario is realized in nature. Finally, we present our discussion and conclusions in Sec. 4.

2 Best Fit Models for Late-Forming Black Holes

Late-forming black holes are parameterized by the injected black hole mass m and fraction f_{Myr} of the DM energy density collapsing into a black hole per unit time (here, 10^6 yrs). The injection rate of black holes is given by $dn/dt_{\text{Myr}} = (\rho_{\text{DM}}/m) f_{\text{Myr}}$, where ρ_{DM} is the DM energy density and time $t_{\text{Myr}} = t/\text{Myr}$. Thus the total number density of injected BH is $n_{\text{BH}} = \tau(m)(\rho_{\text{DM}}/m) f_{\text{Myr}}$, where $\tau(m)$ is the lifetime of the black hole (in Myr) with mass m . Assuming continuous injection of black holes, followed by evaporation with $dM \propto 1/M^2$ leads to a “triangle” distribution, given by $\phi(M) = 3M^2/m^3$ for $M \leq m$ and zero otherwise (see [18, 19] for details). Notice that $\int_0^m \phi(M)dM = 1$. We can rewrite the population of late-forming black holes in terms of the usual f_{PBH} parameter [32] as

$$f_{\text{PBH}} = \frac{n_{\text{BH}}}{\rho_{\text{DM}}} \int_0^m dM M \phi(M) = \frac{3}{4} \tau(m) f_{\text{Myr}}. \quad (2.1)$$

Notice that for $\tau(m) < 1$ the fraction of late-forming black holes in DM is smaller than f_{Myr} , that is injected black hole holes which evaporate on time-scales shorter than a million years contribute a much smaller fraction of the DM than their corresponding injected fraction. This is expected, as the evaporated mass will contribute to the radiation energy density.

Note that while m and f_{Myr} could be constant in the Galaxy with respect to Galactic radius, it is also possible that there is non-trivial DM density dependence on these parameters, such as $f_{\text{Myr}} = f_{0,\text{Myr}}(\rho_{\text{DM}}(r)/\rho_{\text{DM}}(r_{\oplus}))^{p_f}$ and $m = m_0(\phi_{\text{DM}}(r)/\rho_{\text{DM}}(r_{\oplus}))^{p_m}$.

Here $\rho_{\text{DM}}(r_{\oplus})$ is the DM energy density at Earth, and $f_{0,\text{Myr}}, m_0$ are independent of radial distance. It has been shown that the choices $p_f = 1$ and $p_m = 0$ would explain the Galactic center excess morphology [19], and thus we will consider the same parameters for our study.

Generically, black holes with mass M radiate a “primary” particle species i at a rate

$$\frac{\partial^2 N_i^{\text{prim}}}{\partial E_i \partial t} = \frac{g_i}{2\pi} \frac{\Gamma_i(T_{\text{BH}}, E_i, s_i)}{\exp(E_i/T_{\text{BH}}) - (-1)^{s_i}}, \quad (2.2)$$

where g_i are degrees of freedom for particle i , spin s_i , energy E_i , and species dependent gray-body factors Γ_i [32]. In addition to the primary emission $\partial^2 N_i^{\text{prim}}/\partial E_i \partial t$, we also have to take into account the secondary emission $\partial^2 N_i^{\text{secondary}}/\partial E_i \partial t$ from hadronization and decays of unstable states. We utilize the output primary and secondary emission rates from the state-of-the-art `BlackHawk` code [33]. The total emission rate for stable species i , $\partial^2 N_i/\partial E_i \partial t$ is given by the addition of primary and secondary emission rates for that species.

Late-forming MSBHs in the Galactic center radiate photons, and the expected gamma-ray flux is

$$E_\gamma^2 \frac{d\Phi_\gamma}{dE_\gamma} = \tau(m) \left(E_\gamma^2 \int_0^m dM \phi(M) \frac{d^2 N_\gamma}{dE_\gamma dt} \right) \left(\int_{\Delta\Omega} \frac{d\Omega}{4\pi} \int_{\text{l.o.s}} dr \frac{\rho_{\text{DM}}(r)}{m} f_{\text{Myr}}(r) \right), \quad (2.3)$$

where $\Delta\Omega$ for region of interest. For DM density distribution we assume a NFW profile [34],

$$\rho_{\text{DM}}(r) = \frac{\rho_0 r_s^3}{r_s (r_s + r)^2}, \quad (2.4)$$

with $r_s = 25$ kpc, distance to Earth $d = 8.33$ kpc, and energy density at Earth $\rho_{\text{DM}}(r_{\oplus}) = 0.3 \text{ GeV cm}^{-3}$. To find the parameter space in $m, f_{0,\text{Myr}}$ that would explain the Galactic center excess, we use three different datasets each with different background modeling. The dataset from [8, 9] considers region of $2^\circ \leq |l|, |b| \leq 10^\circ$ towards Galactic center for their analysis, whereas [10] uses $|l| \leq 20^\circ, 2^\circ \leq |b| \leq 20^\circ$ and [11] considers $|l|, |b| \leq 40^\circ$. In Fig. 1 We show 68%, 95% confidence interval for these datasets using red, blue, and black contours respectively.

The emission of quarks and gluons from MSBHs also leads to hadronization and thus production of hadrons and, in particular, antiprotons. The flux of antiprotons at Earth depends both on the emission rate and on the subsequent processes of diffusion and energy loss. The resulting antiproton flux detected at Earth, ignoring the background flux, is given by

$$\frac{d\Phi_{\bar{p}}(K, r_{\oplus})}{dK} = \frac{v_{\bar{p}}}{4\pi} \frac{\rho_{\text{DM}}(r_{\oplus})}{m} f_{0,\text{Myr}} R(K) \int_0^m dM \phi(M) \frac{d^2 N_{\bar{p}}}{dK dt}, \quad (2.5)$$

where $K = E - m_p$ is the kinetic energy of \bar{p} , $v_{\bar{p}}$ is velocity, and $R(K)$ factor contains details of propagation. We take $R(K)$ and its error bars from [35], for a DM NFW profile. The flux detected at Earth is further modified by solar modulation, and is

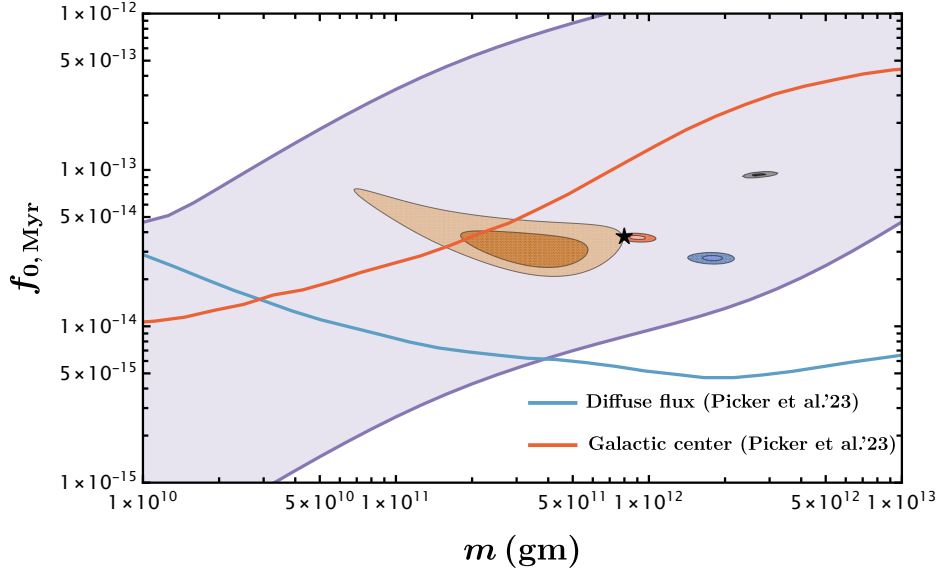


Figure 1: Best fit regions to explain Galactic center excess (red, blue, and black contours), antiproton excess (brown contours), and ${}^3\bar{\text{He}}$ detection (purple contour) in parameter space of injected BH mass m and injected BH fraction $f_{0,\text{Myr}}$. The red [8, 9], blue [10], and black contours [11] are analyses done with different background subtracted models for Galactic center excess. The antiproton excess analysis uses the background model from [15]. For anti-helium excess analysis, we take the detection of 1 event in 10 years at the kinetic energy of $K = 12 \text{ GeV/n}$ [17]. The back star ($8 \times 10^{11} \text{ gm}$, 3.8×10^{-14}) shows our benchmark point. We also show the current best constraint on the late-forming black holes from diffuse extra-galactic gamma-ray and x-ray flux (blue curve) and gamma rays from the Galactic center (red curve) [18]. Although the diffuse background constraints are model dependent and assume injection of BH at higher redshift [18, 19].

given by

$$\frac{d\Phi_{\bar{p}}(K_{\oplus}, r_{\oplus})}{dK_{\oplus}} = \frac{p_{\oplus}^2}{p^2} \frac{d\Phi_{\bar{p}}(K, r_{\odot})}{dK}, \quad K = K_{\oplus} + |Ze|\phi_F, \quad (2.6)$$

where $p = \sqrt{2m_p K + K^2}$ is the momentum, $|Ze|$ is the electric charge of the particle (here $Z = 1$), and $\phi_F = 0.5 \text{ GV}$ is the Fisk potential [35]. Here, K_{\oplus}, p_{\oplus} are the kinetic energy and momentum of the particle after antiprotons reach Earth. In addition to the antiprotons from late-forming black holes, we also expect the astrophysical processes to produce an antiproton background. We consider the background model of Ref. [15] and excess data from [36] for our analysis. The brown contours in Fig.1 show the 68% and 95% C.L. regions in the parameter space when fitting for the possible antiproton excess.

In addition to protons and neutrons from hadronization, higher atomic elements could also be produced from BH evaporation. In particular, in view of the reported tentative AMS-02 events, here we focus on ${}^3\bar{\text{He}}$. The production spectra of ${}^3\bar{\text{He}}$ from an elementary particle i which undergoes hadronization to produce nucleons p, n , can

be estimated using the coalescence model [16, 37]

$$\frac{dN_{3\bar{\text{He}}}^i}{dE_{3\bar{\text{He}}}} = \frac{m_{3\bar{\text{He}}}}{m_p^2 m_n} 3 \left(\frac{p_0^3}{8p_{3\bar{\text{He}}}} \right)^2 \left(\frac{dN_{\bar{p}}^i}{dE_{\bar{p}}} \right)^2 \frac{dN_{\bar{n}}^i}{dE_{\bar{n}}}, \quad (2.7)$$

where $p_0 = 0.246 \pm 0.038$ GeV is coalescence momentum for ${}^3\bar{\text{He}}$ production [17], and $E_{3\bar{\text{He}}}, p_{3\bar{\text{He}}}, m_{3\bar{\text{He}}}$ are, respectively, the energy, momentum and mass of the ${}^3\bar{\text{He}}$ nucleus. Here, $dN_{\bar{p}/\bar{n}}/dE_{\bar{p}/\bar{n}}$ are the antiproton and antineutron spectra at production (thus prior to diffusion and energy losses) from hadronization. The net production rate of ${}^3\bar{\text{He}}$ is then the convolution of the production rate of the elementary particle i with the spectra of ${}^3\bar{\text{He}}$ evaluated from the coalescence equation of Eq. (2.7) i.e.

$$\frac{d^2 N_{3\bar{\text{He}}}}{dE_{3\bar{\text{He}}} dt} = \sum_i \int dE'_i \frac{d^2 N_i}{dE'_i dt} \frac{dN_{3\bar{\text{He}}}^i(E_{3\bar{\text{He}}}, E'_i)}{dE_{3\bar{\text{He}}}}, \quad (2.8)$$

where the variable of integration E'_i is the energy of elementary particle i . In addition to the production rate, again, one needs to take into account diffusion, transport, and solar modulation in order to estimate the flux at the Earth surface. We follow the procedure of Ref. [16] for these estimates. The purple region in Fig. 1 shows the parameter space explaining 1 event in 10 years at $K_{3\bar{\text{He}}} = 12$ GeV/n. The large error bars are a result of huge uncertainty on the coalescence momentum, the transport properties, and the lack of data. Scaling for a larger number of events simply and trivially shifts the contours to larger values of $f_{0,\text{Myr}}$.

In addition to the contours explaining various excess, we also show current best *constraints* on this parameter space coming from gamma rays from the Galactic center (red curve) and diffuse gamma-ray and x-ray flux (blue curve) [19]. The diffuse flux constraints here assume the formation of late-forming MSBHs at much higher redshift and thus are model-dependent.

While our results show a broad range of MSBH masses compatible with multiple excesses, we do find one particular *benchmark point* (shown as a black star in the figure) that would actually explain *all three excesses at once*, at least with the Galactic center signal extracted by the Fermi-LAT Collaboration analyses of Ref. [8, 9]. The benchmark point corresponds to $m = 8 \times 10^{11}$ gm and $f_{0,\text{Myr}} = 3.8 \times 10^{-14}$. We note that the benchmark point corresponds to a lifetime of $\tau(m) \simeq 2.3 \times 10^8$ sec, or around 7 years, and the corresponding spawning rate is of about 5 black holes per cubic parsec per Myr, or around 5,000 black holes per cubic kiloparsec per year. We use this benchmark point for our predictions for other indirect detection signals, with different particle messengers, in the following Sec.3.

3 Model Predictions: antideuterons, positrons, neutrinos, and gamma rays

In this section we use the best-fit, benchmark point discussed above, providing a potential tripartite fit to three indirect detection excesses to estimate the spectrum and

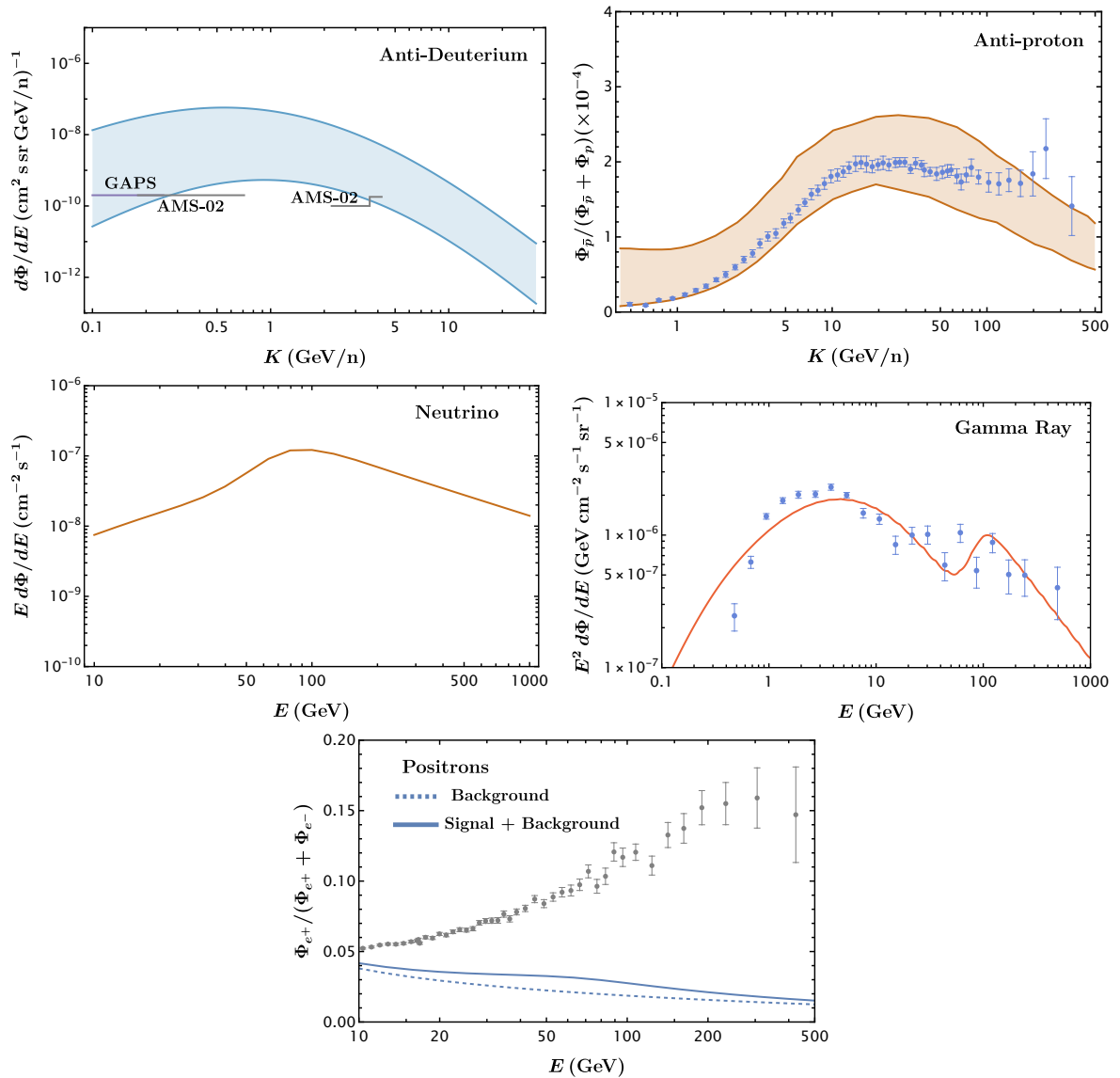


Figure 2: Prediction for the antideuteron flux, antiproton fraction, neutrino flux, gamma-ray flux from the Galactic center, and positron ratio, for the benchmark point shown as a black star in Fig.1. For antideuterons, in the top-left panel, we show the sensitivity limits for GAPS (purple) and AMS-02 (gray) experiments [38, 39]. The top right panel shows the antiprotons fraction, with the observed data points shown with the error bars [36]. In the middle left panel, we show the flavor averaged neutrino flux. The middle right panel compares the expected gamma-ray spectrum for the benchmark point with the observed GCE excess, where the data points with error bars are taken from the analysis done in [8, 9]. In the bottom panel, we compare the expected positron fraction from our model with the observed data points taken from [12], and we take the background model from [40, 41].

expected number of events for positrons, antideuterons (\bar{D} s), and neutrinos. We will also comment on the positron excess.

Similar to the case of ${}^3\bar{\text{H}}\text{e}$ discussed above, the antideuteron production from evaporating BHs (first computed in Ref. [42]) is estimated using a coalescence model, here

$$\frac{dN_{\bar{D}}^i}{dE_{\bar{D}}} = \frac{m_{\bar{D}}}{m_{\bar{p}} m_{\bar{n}}} \left(\frac{p_0^2}{6 p_{\bar{D}}} \right) \frac{dN_{\bar{p}}^i}{dE_{\bar{p}}} \frac{dN_{\bar{n}}^i}{dE_{\bar{n}}}, \quad (3.1)$$

$$\frac{d^2 N_{\bar{D}}}{dE_{\bar{D}} dt} = \sum_i \int dE'_i \frac{d^2 N_i}{dE'_i dt} \frac{dN_{\bar{D}}^i(E_{\bar{D}}, E'_i)}{dE_{\bar{D}}}. \quad (3.2)$$

For the coalescence momentum we adopt $p_0 = 0.192 \pm 0.030$ GeV [17]. For the \bar{D} diffusion, transport, and solar modulation we follow, again, [35]. In Fig. 2 top left panel, we show prediction for \bar{D} spectra for our benchmark point, taking into account the uncertainty in coalescence momentum and transport properties. We also show the sensitivity limits of AMS-02 and GAPS experiments for \bar{D} detection [38, 39, 43] with purple and gray lines, respectively. We deduce that a significant antideuteron flux is expected both at AMS-02 and GAPS, if this scenario for the contemporaneous fit of the three excesses is indeed realized in nature.

In the middle left panel of Fig.2, we show the expected spectra for neutrinos, averaging over flavors, from the Galactic center from the region $|l|, |b| < 10^\circ$. Using the effective area ~ 1 cm² for a 100 GeV neutrino [44], and runtime of 10 yrs $\approx 10^8$ sec, we expect $\mathcal{O}(10)$ events in IceCube detector, significantly smaller compared to the astrophysical backgrounds from atmospheric neutrinos [44].

In the bottom panel of Fig.2, we show the expected spectra for positrons for our benchmark point. For diffusion and energy loss equations, we again rely on the analysis from [35]. For the background model, we use the analytical forms of [40, 41]. We can see that the predicted signal is significantly below the observed positron excess [12].

In the top right panel, we show the comparison of the observed antiproton *fraction* [36], with what is expected from our benchmark model. We have also added the antiproton background model and its uncertainty from [15]. This indicates that the model is broadly consistent with observations, albeit in marginal tension at low energies. Finally, in the middle right panel, we show the comparison of gamma-ray flux from the Galactic center from our benchmark model with the background-subtracted data from the Fermi Collaboration analysis [8, 9].

4 Discussion and Conclusions

We have studied the tantalizing possibility that three long-standing anomalies – the Galactic center gamma-ray excess, the antiproton excess, and the tentative anti-helium 3 events reported by the AMS-02 Collaboration, may all originate from late-spawned, light black holes of non-stellar origin. We find that in order to fit the three putative signals, such black holes must have a mass of around 10^{12} gm (and thus a lifetime of

about ten years) and be injected at a rate of around 5 black holes per cubic parsec per mega-year.

To cross-constrain this scenario, we explored the implications for “orthogonal” astrophysical messengers, such as antideuterons, positrons, and neutrinos, that also necessarily arise from the evaporation of the late-forming black holes. We found that by and large an antideuteron signal is slated to appear, if this scenario is realized in nature, both at AMS-02 and at GAPS; the predictions for the high-energy neutrino flux are far below the atmospheric neutrino background, and the positron flux is also small compared to the observed high-energy cosmic-ray positron flux.

In conclusion, this scenario, unlike the numerous DM-related scenarios posited to explain some of the excess under scrutiny here, is highly predictive, as black hole evaporation is a universal process, given a black hole mass function and spin distribution, and assuming no “dark” degrees of freedom. As such, we were able to produce concrete predictions for the spectra of multiple messengers, in addition to providing a remarkably good fit to the observed signals. Above all, the advent of GAPS, and future measurements of the antideuteron flux with AMS-02, will conclusively probe the scenario under consideration here.

Acknowledgments

We thank Mattia Di Mauro Philip Von Doetinchem. S.P. is partly supported by the U.S. Department of Energy grant number de-sc0010107. M.K. acknowledges support from the National Science Foundation (Grant No. PHY-2020275).

References

- [1] **Particle Data Group** Collaboration, R. L. Workman et al., *Review of Particle Physics*, *PTEP* **2022** (2022) 083C01.
- [2] G. Arcadi, M. Dutra, P. Ghosh, M. Lindner, Y. Mambrini, M. Pierre, S. Profumo, and F. S. Queiroz, *The waning of the WIMP? A review of models, searches, and constraints*, *Eur. Phys. J. C* **78** (2018), no. 3 203, [[arXiv:1703.07364](#)].
- [3] G. Arcadi, D. Cabo-Almeida, M. Dutra, P. Ghosh, M. Lindner, Y. Mambrini, J. P. Neto, M. Pierre, S. Profumo, and F. S. Queiroz, *The Waning of the WIMP: Endgame?*, [arXiv:2403.15860](#).
- [4] T. R. Slatyer, *Les Houches Lectures on Indirect Detection of Dark Matter*, *SciPost Phys. Lect. Notes* **53** (2022) 1, [[arXiv:2109.02696](#)].
- [5] **Fermi-LAT** Collaboration, W. B. Atwood et al., *The Large Area Telescope on the Fermi Gamma-ray Space Telescope Mission*, *Astrophys. J.* **697** (2009) 1071–1102, [[arXiv:0902.1089](#)].
- [6] L. Goodenough and D. Hooper, *Possible Evidence For Dark Matter Annihilation In The Inner Milky Way From The Fermi Gamma Ray Space Telescope*, [arXiv:0910.2998](#).

- [7] D. Hooper and L. Goodenough, *Dark Matter Annihilation in The Galactic Center As Seen by the Fermi Gamma Ray Space Telescope*, *Phys. Lett. B* **697** (2011) 412–428, [[arXiv:1010.2752](#)].
- [8] **Fermi-LAT** Collaboration, M. Ajello et al., *Fermi-LAT Observations of High-Energy γ -Ray Emission Toward the Galactic Center*, *Astrophys. J.* **819** (2016), no. 1 44, [[arXiv:1511.02938](#)].
- [9] **Fermi-LAT** Collaboration, M. Ackermann et al., *The Fermi Galactic Center GeV Excess and Implications for Dark Matter*, *Astrophys. J.* **840** (2017), no. 1 43, [[arXiv:1704.03910](#)].
- [10] F. Calore, I. Cholis, and C. Weniger, *Background Model Systematics for the Fermi GeV Excess*, *JCAP* **03** (2015) 038, [[arXiv:1409.0042](#)].
- [11] M. Di Mauro, *Characteristics of the Galactic Center excess measured with 11 years of Fermi-LAT data*, *Phys. Rev. D* **103** (2021), no. 6 063029, [[arXiv:2101.04694](#)].
- [12] **AMS** Collaboration, L. Accardo et al., *High Statistics Measurement of the Positron Fraction in Primary Cosmic Rays of 0.5–500 GeV with the Alpha Magnetic Spectrometer on the International Space Station*, *Phys. Rev. Lett.* **113** (2014) 121101.
- [13] M.-Y. Cui, Q. Yuan, Y.-L. S. Tsai, and Y.-Z. Fan, *Possible dark matter annihilation signal in the AMS-02 antiproton data*, *Phys. Rev. Lett.* **118** (2017), no. 19 191101, [[arXiv:1610.03840](#)].
- [14] A. Cuoco, M. Krämer, and M. Korsmeier, *Novel Dark Matter Constraints from Antiprotons in Light of AMS-02*, *Phys. Rev. Lett.* **118** (2017), no. 19 191102, [[arXiv:1610.03071](#)].
- [15] I. Cholis, T. Linden, and D. Hooper, *A Robust Excess in the Cosmic-Ray Antiproton Spectrum: Implications for Annihilating Dark Matter*, *Phys. Rev. D* **99** (2019), no. 10 103026, [[arXiv:1903.02549](#)].
- [16] E. Carlson, A. Coogan, T. Linden, S. Profumo, A. Ibarra, and S. Wild, *Antihelium from Dark Matter*, *Phys. Rev. D* **89** (2014), no. 7 076005, [[arXiv:1401.2461](#)].
- [17] A. Coogan and S. Profumo, *Origin of the tentative AMS antihelium events*, *Phys. Rev. D* **96** (2017), no. 8 083020, [[arXiv:1705.09664](#)].
- [18] Z. S. C. Picker and A. Kusenko, *Constraints on late-forming exploding black holes*, *Phys. Rev. D* **108** (2023), no. 2 023012, [[arXiv:2305.13429](#)].
- [19] Z. S. C. Picker and A. Kusenko, *Explaining the GeV excess with exploding black holes*, *Phys. Lett. B* **845** (2023) 138175, [[arXiv:2305.13434](#)].
- [20] M. Korwar and S. Profumo, *Updated constraints on primordial black hole evaporation*, *JCAP* **05** (2023) 054, [[arXiv:2302.04408](#)].
- [21] S. W. Hawking, *Particle Creation by Black Holes*, *Commun. Math. Phys.* **43** (1975) 199–220. [Erratum: *Commun.Math.Phys.* 46, 206 (1976)].
- [22] K. Kawana, P. Lu, and K.-P. Xie, *First-order phase transition and fate of false vacuum remnants*, *JCAP* **10** (2022) 030, [[arXiv:2206.09923](#)].
- [23] J.-P. Hong, S. Jung, and K.-P. Xie, *Fermi-ball dark matter from a first-order phase transition*, *Phys. Rev. D* **102** (2020), no. 7 075028, [[arXiv:2008.04430](#)].

- [24] P. Lu, K. Kawana, and K.-P. Xie, *Old phase remnants in first-order phase transitions*, *Phys. Rev. D* **105** (2022), no. 12 123503, [[arXiv:2202.03439](#)].
- [25] S. Savastano, L. Amendola, J. Rubio, and C. Wetterich, *Primordial dark matter halos from fifth forces*, *Phys. Rev. D* **100** (2019), no. 8 083518, [[arXiv:1906.05300](#)].
- [26] M. M. Flores, A. Kusenko, L. Pearce, and G. White, *Fireball baryogenesis from early structure formation due to Yukawa forces*, *Phys. Rev. D* **108** (2023), no. 9 L091705, [[arXiv:2208.09789](#)].
- [27] M. M. Flores and A. Kusenko, *Primordial Black Holes from Long-Range Scalar Forces and Scalar Radiative Cooling*, *Phys. Rev. Lett.* **126** (2021), no. 4 041101, [[arXiv:2008.12456](#)].
- [28] G. Domènech, D. Inman, A. Kusenko, and M. Sasaki, *Halo formation from Yukawa forces in the very early Universe*, *Phys. Rev. D* **108** (2023), no. 10 103543, [[arXiv:2304.13053](#)].
- [29] A. Chakraborty, P. K. Chanda, K. L. Pandey, and S. Das, *Formation and Abundance of Late-forming Primordial Black Holes as Dark Matter*, *Astrophys. J.* **932** (2022), no. 2 119, [[arXiv:2204.09628](#)].
- [30] P. Lu, K. Kawana, and A. Kusenko, *Late-forming primordial black holes: Beyond the CMB era*, *Phys. Rev. D* **107** (2023), no. 10 103037, [[arXiv:2210.16462](#)].
- [31] K. Kawana and K.-P. Xie, *Primordial black holes from a cosmic phase transition: The collapse of Fermi-balls*, *Phys. Lett. B* **824** (2022) 136791, [[arXiv:2106.00111](#)].
- [32] B. Carr, K. Kohri, Y. Sendouda, and J. Yokoyama, *Constraints on primordial black holes*, *Rept. Prog. Phys.* **84** (2021), no. 11 116902, [[arXiv:2002.12778](#)].
- [33] A. Arbey and J. Auffinger, *BlackHawk: A public code for calculating the Hawking evaporation spectra of any black hole distribution*, *Eur. Phys. J. C* **79** (2019), no. 8 693, [[arXiv:1905.04268](#)].
- [34] J. F. Navarro, C. S. Frenk, and S. D. M. White, *The Structure of cold dark matter halos*, *Astrophys. J.* **462** (1996) 563–575, [[astro-ph/9508025](#)].
- [35] M. Cirelli, G. Corcella, A. Hektor, G. Hutsi, M. Kadastik, P. Panci, M. Raidal, F. Sala, and A. Strumia, *PPPC 4 DM ID: A Poor Particle Physicist Cookbook for Dark Matter Indirect Detection*, *JCAP* **03** (2011) 051, [[arXiv:1012.4515](#)]. [Erratum: *JCAP* 10, E01 (2012)].
- [36] **AMS** Collaboration, M. Aguilar et al., *Antiproton Flux, Antiproton-to-Proton Flux Ratio, and Properties of Elementary Particle Fluxes in Primary Cosmic Rays Measured with the Alpha Magnetic Spectrometer on the International Space Station*, *Phys. Rev. Lett.* **117** (2016), no. 9 091103.
- [37] A. Ibarra and S. Wild, *Prospects of antideuteron detection from dark matter annihilations or decays at AMS-02 and GAPS*, *JCAP* **02** (2013) 021, [[arXiv:1209.5539](#)].
- [38] **GAPS** Collaboration, T. Aramaki, C. J. Hailey, S. E. Boggs, P. von Doetinchem, H. Fuke, S. I. Mognet, R. A. Ong, K. Perez, and J. Zweerink, *Antideuteron Sensitivity for the GAPS Experiment*, *Astropart. Phys.* **74** (2016) 6–13, [[arXiv:1506.02513](#)].

- [39] T. Aramaki et al., *Review of the theoretical and experimental status of dark matter identification with cosmic-ray antideuterons*, *Phys. Rept.* **618** (2016) 1–37, [[arXiv:1505.07785](#)].
- [40] E. A. Baltz and J. Edsjo, *Positron propagation and fluxes from neutralino annihilation in the halo*, *Phys. Rev. D* **59** (1998) 023511, [[astro-ph/9808243](#)].
- [41] M. Cirelli, R. Franceschini, and A. Strumia, *Minimal Dark Matter predictions for galactic positrons, anti-protons, photons*, *Nucl. Phys. B* **800** (2008) 204–220, [[arXiv:0802.3378](#)].
- [42] A. Barrau, G. Boudoul, F. Donato, D. Maurin, P. Salati, I. Stefanon, and R. Taillet, *Antideuterons as a probe of primordial black holes*, *Astron. Astrophys.* **398** (2003) 403–410, [[astro-ph/0207395](#)].
- [43] V. Choutko and F. Giovacchini, *Cosmic Rays Antideuteron Sensitivity for AMS-02 Experiment*, in *International Cosmic Ray Conference*, vol. 4 of *International Cosmic Ray Conference*, pp. 765–768, Jan., 2008.
- [44] A. Karle, *IceCube*, *arXiv e-prints* (Mar., 2010) arXiv:1003.5715, [[arXiv:1003.5715](#)].